Pramāṇa, Vol. 1, No. 1, 1973. Printed in India.

Atmospheric gamma rays in the energy region 40–1000 GeV

K C ANAND, R R DANIEL and S A STEPHENS
Tata Institute of Fundamental Research, Bombay 400005

MS received 5 May 1973

Abstract. A large stack of lead-emulsion sandwich detector assembly was flown over Hyderabad, India. High energy gamma rays at the float altitude were unambiguously identified from the cascades they induced, and their energies reliably determined by improved methods. From an analysis of 163 gamma rays of energy $\gtrsim$ 30 GeV, it is found that the differential energy spectrum is represented by the power law $J_\gamma(E) = 129{\cdot}4E^{-2{\cdot}62\pm0{\cdot}12}$ photons m^{-2} $sr^{-1}sec^{-1}$ GeV^{-1} at an effective atmospheric depth of 14·3 g cm^{-2}; this is the first reliable balloon measurement of atmospheric gamma rays in the energy range 40-1000 GeV. After correcting for the gamma rays radiated by the primary cosmic ray electrons, the production spectrum of gamma rays, resulting from the collisions of cosmic ray nuclei with air nuclei, at the top of the atmosphere is $P_\gamma(E, 0) = 8{\cdot}02 \times 10^{-4}\ E^{2{\cdot}60\pm0{\cdot}09}$ photons $g^{-1}sr^{-1}sec^{-1}$ GeV^{-1}. The atmospheric propagation of the electromagnetic component due to the cascade process is also derived from the gamma ray production spectrum.

Keywords. Gamma rays; cascade process; production spectrum; cosmic rays.

1. Introduction

We know that a study of gamma rays sampled at small atmospheric depths, reveals information on the characteristics of high energy interactions. Further, since at energies greater than a few GeV almost all secondary electrons at small atmospheric depths are due to the materialisation of gamma rays, the only reliable method of estimating the secondary electron spectrum, which in turn is essential to deduce the spectrum of primary cosmic ray electrons from balloon experiments, is from a direct determination of the atmospheric gamma ray spectrum at similar altitudes. Therefore, an experiment has been carried out using a lead-emulsion sandwich stack, which was exposed over Hyderabad, India, under 10·3 g cm^{-2} of residual atmosphere. Preliminary results from this experiment using a total of 103 gamma rays of energy $\gtrsim$ 90 GeV were reported at the International Cosmic Ray Conference at Hobart (Anand *et al* 1971). In the present paper, we give the final results using 163 gamma rays of energy $\gtrsim$ 35 GeV.

2. Experimental details

2.1. *Detector assembly and the balloon flight*

The detector system used here is a horizontal lead-emulsion sandwich assembly (Anand

et al 1970), consisting of an upper block of pure emulsions 1·8 cm thick having 30 Ilford G-5 pellicles, followed by 16 alternate layers of 600 μm thick G-5 pellicles and lead sheets; the top lead sheet was 1 mm thick followed by 9 of 2 mm and 6 of 3 mm (figure 1). The detector assembly had an area of 45 cm $\times$ 30 cm and had a total depth of 8·3 radiation lengths (r.l). While the upper emulsion block preserved the very distinct advantages of a pure emulsion stack for unique identification of gamm ray events, the lead-emulsion sandwich, in which the electromagnetic cascades develop rapidly, served as the detector and energy discriminator.

The above unit weighing about 100 kg was flown horizontally in a balloon launched from Hyderabad, India (vertical geomagnetic threshold rigidity 16·9 GV) on May 4, 1968. The assembly was flipped through 180° when the balloon reached the ceiling altitude, whereafter it floated at a constant altitude of 10·3 mb for a duration of 352 minutes. The flipping of the assembly permits the rejection of all events recorded during the period of ascent of the balloon. The detector assembly was stored in the inverted position before the flight, and the emulsion layers were reshuffled immediately after the flight.

2.2. *Microscope scanning and identification of events*

Each emulsion plate was cut into three parts of equal size 15 cm $\times$ 30 cm; they are referred to as A, B and C series. Systematic and careful microscope scanning of emulsions was carried out under a total magnification of X 225 at two depths, for events with more than about 5 tracks within an equivalent circle of diameter 100 μm and having zenith angles between 15° and 65°. As shown in figure 1, the scanning was first carried out at a depth of 3·2 r.l (Scan I—Layer I) and the second at a depth of 2·4 r.l (Scan II—Layer II). All events obtained in Scan I were traced up through successive emulsions and those originating as electron pairs in the pure emulsion block, and moving down with no associated parallel track, were identified as due to gamma rays. In the case of events from Scan II, only those which were not picked up in Scan I were traced towards the pure emulsion block. In this manner a total of 257 gamma ray events were identified.

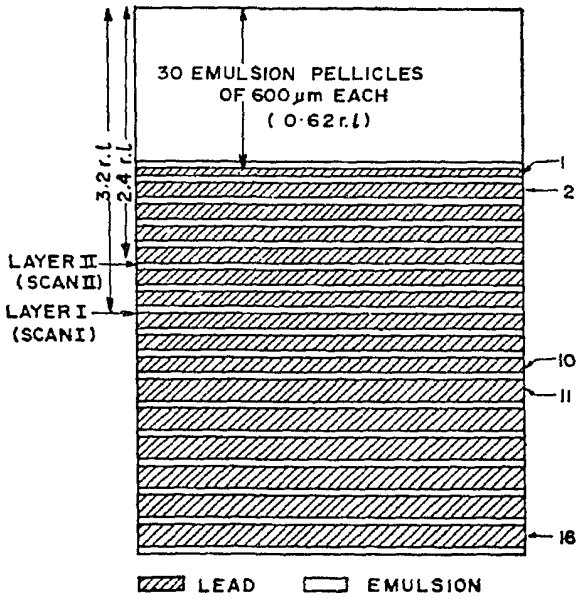

Figure 1. Schematic drawing of the emulsion-lead sandwich assembly. Layers marked I and II correspond to the emulsion plates in which the first and second scannings were respectively carried out.

2.3. *Energy estimation*

In our earlier experiments (Anand *et al* 1968; Stephens 1970) we estimated the energy of the gamma rays by comparing the number of tracks at the cascade maximum in the detector assembly with that expected on the basis of theoretical calculations of Kidd and Nishimura (1964). Experimentally, the number of tracks at the cascade maximum was obtained from the smooth transition curve constructed by using the visual counts of the number of tracks within a circle of suitable radius, r, about the cascade axis at various depths in the detector. Two experimental criteria adopted in counting tracks at each depth were: (i) the tracks should have angles $\leqslant 10°$ with respect to the shower axis; and (ii) the shower axis is defined by the weighted centre of the tracks constituting the core of the cascade.

However, it has been pointed out by Anand and Stephens (1971) that in our experiment, as also in many others, the use of the theoretical calculations of Kidd and Nishimura (1964) leads to systematic errors in the energy estimation, since the experimental criteria followed do not match with the requirements of the theoretical calculations, namely: (a) the calculations relate to the number of tracks of *all angles* with respect to the shower axis in a circle of given radius r; (b) the incident direction of the gamma ray defines the axis of the cascade; and (c) the detector assembly can be approximated by a homogeneous medium with a suitable radiation length for propagating the cascade. None of the three conditions apply to our experiment. (Our calculations reveal in the case of events at the low energy end of our study that the centroid of all tracks is sometimes found to be displaced from the incident gamma ray direction by distances comparable to the radius of the circle used for counting the tracks). In order to overcome these shortcomings we have made new and rigorous calculations for computing the number of tracks at the cascade maximum by simulating gamma ray initiated showers by Monte Carlo method for the actual detector configuration and incorporating all experimental criteria. The present calculations are made for gamma rays of energies 30, 50, 100, 200 and 500 GeV. The number of tracks at the cascade maximum were then determined from the smoothened transition curve constructed from these calculations in a manner identical to the experimental procedure. In figure 2, we show our calculated most probable number of tracks within a circle of radius 68 μm at the maximum in the transition curve, as a function of the gamma ray energy.

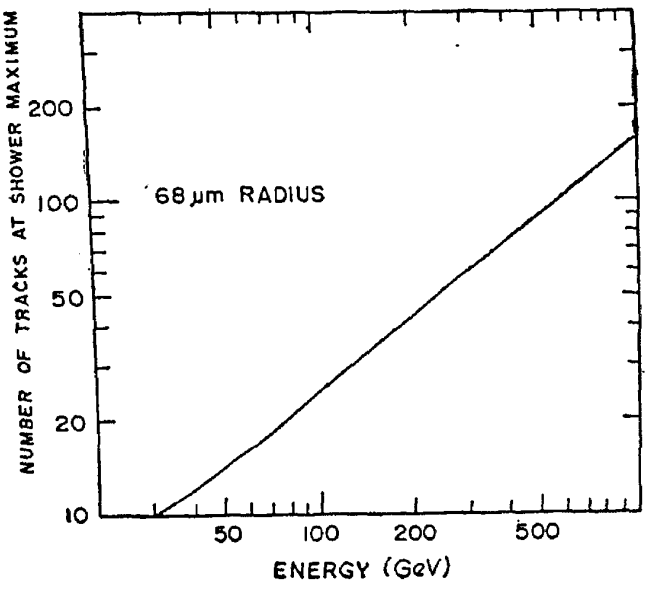

Figure 2. The calculated number of electron tracks at the cascade maximum making angles $<10°$ to the direction of the primary, and lying within a circle of radius 68 μm about the weighted centre of the tracks, plotted against gamma ray energy.

From a comparison of the energy estimates derived from the present calculations and those of Kidd and Nishimura (1964) as a function of energy, it is noticed that the calculations of the latter applied to our experiment lead to a systematic overestimation amounting to 35 per cent at about 30 GeV, gradually decreasing to 15 per cent at about 100 GeV; beyond 200 GeV, their calculations predict systematically lower energies, the underestimation at about 500 GeV being about 10 per cent. This effect can be understood as follows: At all energies experimental criterion (i) leads to the rejection of a few tracks with angles $>10°$ to the axis and therefore to lower energy estimates. However, at low energies, i.e. <100 GeV, there are two effects both compensating for this underestimation. Of these, the first is due to criterion (ii) and the second to the large fluctuations in the position of the cascade maximum leading to a higher number of tracks at the maximum for an individual cascade compared to that for the average case.

In the present experiment, we have made use of the curve in figure 2 obtained from our calculations to determine the energy of the cascade. In view of the extensive improvements we have introduced in the calculations, we expect no further systematic error remaining in our energy estimation. The error due to statistical fluctuations is found to be about 25 per cent irrespective of the energy within the range we are concerned here.

2.4 *Detection Probability*

The probability of observing an event during the microscope examination of the nuclear emulsions will depend on the detection probability defined by the minimum number of tracks $n_L^{\,i}$ in the scan layer as required by the observer, and his scanning efficiency. However, the final selection of events will also depend on the angular

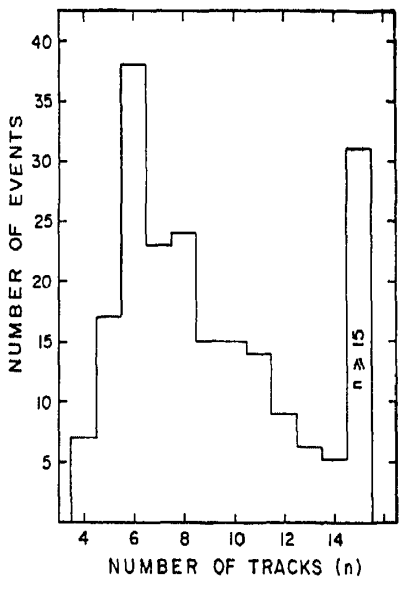

Figure 3. The observed distribution of events having a number of tracks n within a circle of radius 28 μm is shown for events recorded in B-series during the Scan II at Layer II.

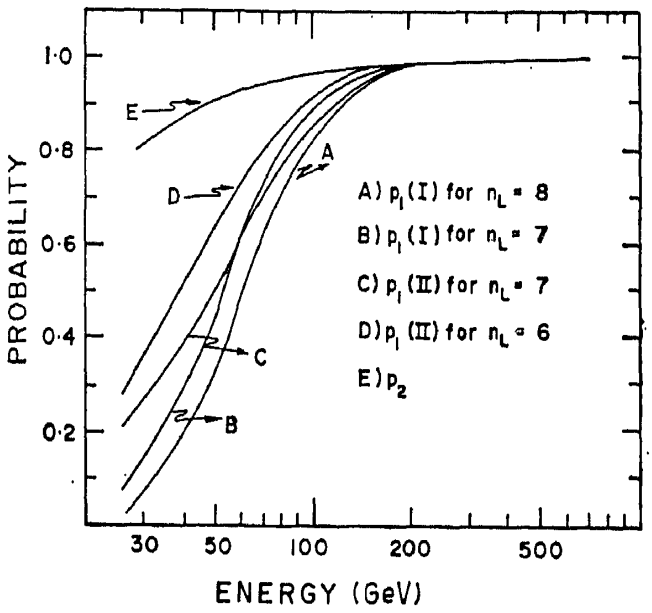

Figure 4. Curves A & B are the probabilities for detecting an event in Layer I for two different values of n_L; Curves C & D are those in Layer II. Curve E is the probability to see at least two parallel tracks within 10° to each other and displaced by a distance less than 56 μm in the lowermost emulsion pellicle of the pure emulsion stack.

Table 1. Pick-up criteria for scanning and the scanning efficiency

Scan	n_L			Scanning efficiency, per cent		
	A-series	B-series	C-series	70–125 GeV	125–200 GeV	>200 GeV
Scan I	7	7	8	70 ± 10	83 ± 15	96^{+4}_{-20}
Scan II	7	6	7	84 ± 8	84 ± 9	100

and energy acceptance criteria employed. In this section we will consider only the former, i.e. the detection probability; the angular and energy acceptance criteria and the scanning efficiency will be considered in sections 2·5 and 2·6 respectively.

The detection probability for gamma ray initiated cascades depends upon: (i) the minimum number of tracks n_L as required by the observer while scanning for the event; (ii) the energy of the gamma ray; and (iii) the depth at which the scanning is made. In order to determine rquirement (i) quantitatively, we measured the number of tracks n within a circle of radius 28 μm at Layers I and II for all identified events obtained in Scans I and II. In figure 3 we show a typical distribution of the number of tracks at Layer II of all events (electron and gamma ray initiated events) obtained from the B-series during Scan II. One can see from the histogram that for $n<6$, there is a significant drop in the efficiency of detection of events. We therefore set $n_L=6$ tracks for the B-series of Scan II. Identical procedures were followed for all the other scans and we present in table 1, the values of n_L for different scans and for different series.

Knowing the value of n_L one can determine the probability p_1 of finding atleast n_L tracks in the scan plate provided the number distribution of tracks at a given depth is available for a given energy. For this purpose detailed Monte Carlo calculations were carried out (Anand and Stephens 1973) to determine the respective probabilities $p_1(\mathrm{I}, E)$ and $p_1(\mathrm{II}, E)$ for the two levels of scanning; the results are shown in figure 4 for values of n_L listed in table 1. One can see from this figure that in all cases p_1 decreases sharply below 100 GeV and that Scan II is more favourable for scanning at low energies compared to larger depths.

While tracing the events from the sandwich section of the assembly into the pure emulsion section, it was found necessary to demand at least two associated tracks separated by distances less than 56 μm and making angles less than 10° with one another in the lowest pellicle of the pure emulsion block, so that there will be 100 per cent efficiency in tracing events into the pure emulsion block. It is therefore necessary to calculate the probability p_2 of such occurrences as a function of energy. From the Monte Carlo calculations already mentioned, we show in figure 4 the variation of p_2 with energy. The condition that the event maintains at least two tracks upto the scanning layer was found to be always satisfied. One can see from figure 4 that p_2 is a slowly varying function of energy.

A careful examination of the calculated values of $p_1(\mathrm{I}, E)$, $p_1(\mathrm{II}, E)$ and p_2, reveals that they are nearly independent of one another.

2.5. *Angular and Energy acceptance criteria*

One can see from figure 4 that at energies below about 60 GeV, the detection pro-

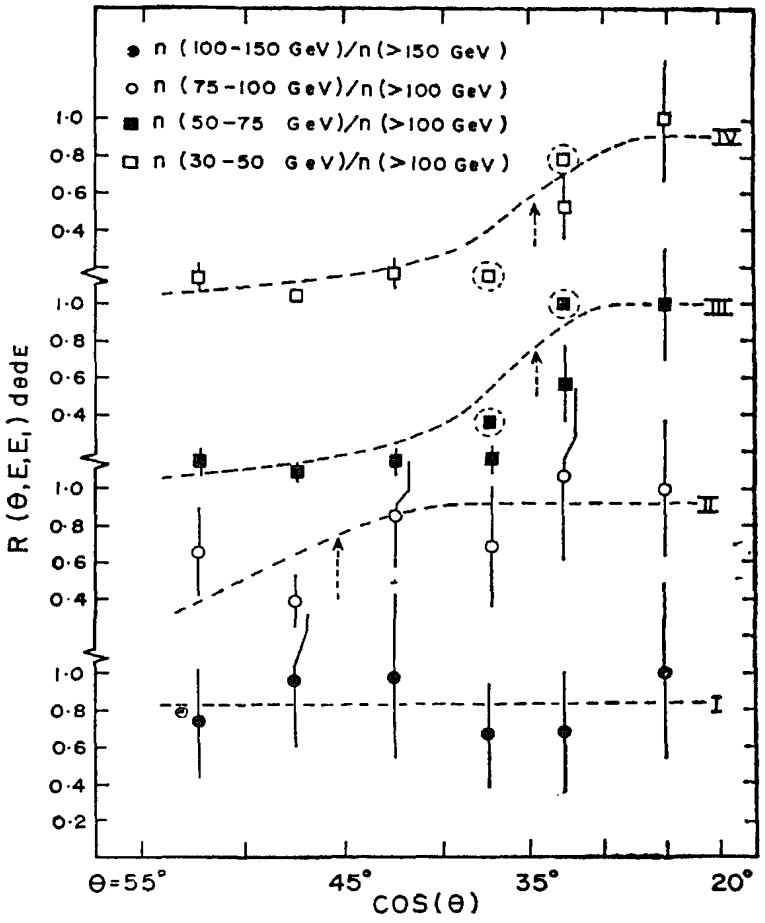

Figure 5. The ratio R of the number of events having energy between E and $E+\mathrm{d}E$ and zenith angles between θ and $\theta+\mathrm{d}\theta$ to the number above energy E_1 in the same angular interval is plotted as a function of cos θ, for different energy intervals; the points marked within dotted circles are based on the events obtained in B-series only.

bability p_1 decreases as the depth in the assembly increases; it therefore follows that as the zenith angle of the event increases, p_1 decreases further. Secondly, the type of scanning technique adopted by us, namely the rapid movement of vertical focussing, made the scanning less efficient for events with low energies and large zenith angles. In order to assess the magnitude of these effects, we have examined the variation with cos θ, of the ratio $R(\theta, E, E_1)\mathrm{d}\theta\mathrm{d}E$; here the quantity R is defined as the ratio of the number of events with energy E and angle θ within the intervals $\mathrm{d}E$ and $\mathrm{d}\theta$ respectively, to the total number of events of energy greater than a suitable value E_1 above which p_1 and p_2 are close to unity but in the same angular interval. For the sake of convenience the ratios calculated for $\theta=20°$-$30°$ are taken to be unity; the final values are summarized in figure 5. From this figure, one can see that for energies >100 GeV, R is independent of θ (curve I). Curve II indicates that events in the range 50–75 GeV show slight dependence on θ for $\theta>40°$. Curves III and IV show that for energies <75 GeV, R decreases sharply above 30° (the points marked with dotted circles are from B-series in which even events with about 20 GeV were picked up with a high degree of efficiency). From an examination of figure 5, we arrived at the angular selection criteria as shown in table 2. Thus, finally we have rejected nearly all events having detection probability $p_1<0{\cdot}5$, avoiding large correction factors.

After taking into account all the criteria described above, we obtained a total of 163 events with energies >35 GeV for the final analysis.

2.6. *Scanning efficiency*

As mentioned in section 2.4, since we have counted the number of tracks within a circle of radius 28 μm for all events observed in Scans I and II, it becomes possible to

Table 2. Zenith angle and minimum energy criteria

Energy interval in GeV	Zenith angle interval	Series	Low energy cut-off E_m	
			Scan I	Scan II
$E_\gamma < 75$	20°–35°	A	70 GeV	50 GeV
$75 \leq E_\gamma < 100$	20°–45°	B	50 GeV	30 GeV
$E_\gamma \geq 100$	20°–60°	C	70 GeV	70 GeV

calculate the scanning efficiency separately for the different scans. The scanning efficiency was found to be independent of the series and as a result, we could combine events initiated by both gamma rays and electrons from all series to determine the scanning efficiency as a function of energy. In table 1, we summarise the efficiencies for three different energy intervals; the higher efficiency for Scan II is probably due to the better care taken during the second scan. The efficiency for energy below 70 GeV could not be determined reliably because of the limited number of events available, after the application of selection criteria described earlier. However, since in Scan II, the efficiency remains the same in the energy intervals 70–200 GeV we assumed this trend to continue at least upto 30 GeV for B-series and upto 50 GeV for A-series. In the case of Scan I in B-series, the dependence of the scanning efficiency on energy, as suggested by the values in table 1, was extrapolated from 70 GeV to 50 GeV.

3. Results

3.1. *Flux and energy spectrum of gamma rays at the float altitude*

In order to determine the flux of gamma rays, one requires: (i) the number of gamma rays incident on the detector assembly for a given energy interval, and (ii) the corresponding geometrical factor. The former was estimated in the following manner. All observed gamma rays were grouped into small energy intervals, and each of these numbers multiplied by a factor $k(E)$ given by

$$\begin{aligned} k^{-1}(E) = &\{p_1(E, \mathrm{I})\,\epsilon(E, \mathrm{I}) + p_1(E, \mathrm{II})\,\epsilon(E, \mathrm{II}) \\ &= p_1(E, \mathrm{I})\,p_1(E, \mathrm{II})\,\epsilon(E, \mathrm{I})\,\epsilon(E, \mathrm{II})\}\, p_2(E) p_3 \end{aligned} \tag{1}$$

where ϵ's are the various scanning efficiencies, and p_3 the probability of materialization of the gamma ray in the pure emulsion block. It may be noted that equation 1 is strictly valid only if the probabilities p_1's are independent of each other; indeed this is found to be true at low energies while at high energies, since these probabilities are close to unity, the above assumption does not lead to any deviation from the true situation (section 2·4). In this manner we determined the total number of gamma rays incident on the detector assembly for different energy intervals.

The geometrical factor at energies $\geqslant$100 GeV, after taking into account the rejection of events entering through the sides and bad regions in the emulsion, is $4{\cdot}19 \times 10^3$ (m^2 sr sec). Since below 100 GeV, the geometrical factor for each energy interval depends also on the selection criteria used (table 2), they were calculated separately. Furthermore, the effective atmospheric depth varies from 14·3 g cm^{-2} at energies $>$100 GeV to 11·7 g cm^{-2} for energies $<$75 GeV; hence we have corrected all flux values below 100 GeV using a depth dependent function,

$$f(x) = 6{\cdot}069 \exp(-x/125{\cdot}0) - 5{\cdot}914 \exp(-x/94{\cdot}4) - 0{\cdot}115 \exp(-x/21{\cdot}64) \tag{2}$$

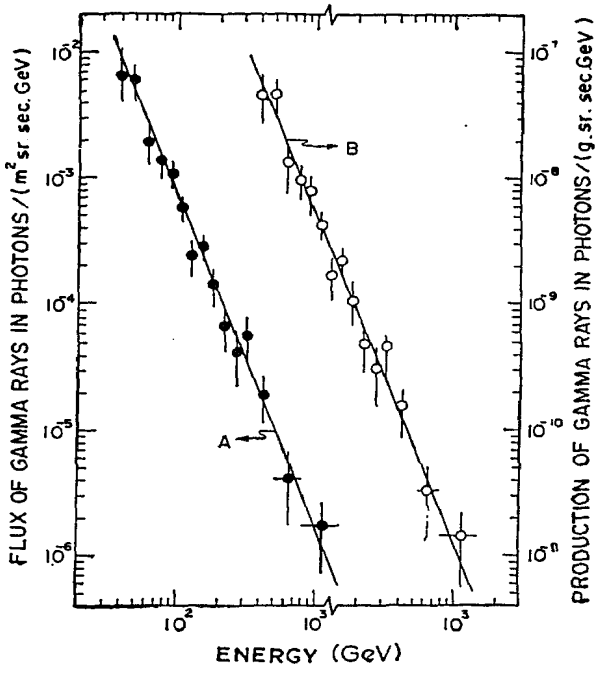

Figure 6. The differential energy spectrum of gamma rays at an effective depth of 14·3 g cm^{-2} is shown in the left hand side, while the production spectrum of gamma rays at the top of the atmosphere is shown on the right hand side.

This function has been derived using the one-dimensional cascade theory (see equation 6b). The corrected flux values are plotted on the left hand side of figure 6; the errors shown in this figure include both statistical and the uncertainties in the calculated probabilities and efficiencies. The differential energy spectrum of the observed gamma rays (Curve I) at an effective depth of 14·3 g cm^{-2} for energies greater than 40 GeV can be represented by a simple power law of the type

$$J_\gamma(E) = 129{\cdot}4E^{-2{\cdot}62\pm0{\cdot}12} \text{ photons (m}^2 \text{ sr sec GeV)}^{-1}$$

Comparison with other available data—Though a number of attempts have been made in the past to study high energy gamma rays in the upper atmosphere, they are usually associated with large statistical errors and/or large systematic errors. However, for the sake of completeness we will now discuss them here. We summarise in table 3, the available information on the spectral shape of the integral energy spectrum. We infer from this table that within the errors quoted, all values are consistent with one another. However, of the four investigations included in table 3, the one due to Nishimura *et al* (1970) gives absolute flux values a factor of two smaller than the present work; here it will be pertinent to remark that while these authors made corrections for scanning efficiency, they have, without justification, assumed the detection probability to be 100 per cent. The results of Kidd (1963a) on the other hand have been revised in a subsequent paper (Abraham *et al* 1963a) in view of the unexplained disagreement between their observations by a factor two. Subsequent to this, these values have been reduced by a factor of 10 (Kidd 1963b; Abraham *et al* 1963b) ! In the experiment of Malhotra *et al* (1965) the production rate of gamma rays was deduced for the top of the atmosphere assuming a mean floating altitude of 22 g cm^{-2} over a total float time of 28 hours of which the altitude for 18 hours was deduced from indirect means when the atmospheric depth is supposed to have varied by as much as 16 to 51 g cm^{-2}. Attention should be drawn here that small changes in float altitude lead to large variations in the derived production spectrum because of the larger

Table 3. Integral spectral index of gamma rays at balloon altitudes

Energy in GeV	Spectral index	Float altitude g cm^{-2}	Reference
500–1500	$2{\cdot}0 \pm 0{\cdot}5$	8	Duthie *et al* (1962)
70–1000	$1{\cdot}9^{+0{\cdot}3}_{-0{\cdot}2}$	6·5	Kidd (1963a); Abraham *et al* (1963a)
370–2650	$1{\cdot}57 \pm 0{\cdot}08$	22	Malhotra *et al* (1965)
50–200	$1{\cdot}8 \pm 0{\cdot}4$	6·0	Nishimura *et al* (1970)
40–1000	$1{\cdot}62 \pm 0{\cdot}12$	10·3	present experiment

geometrical factors involved at larger atmospheric depths. Finally, the measurements due to Duthie *et al* (1962) are associated with very large statistical errors; not only that, in this experiment, as also in that of Malhotra *et al* (1965) the flux values include gamma rays and electrons since experimentally it is not possible to separate the two. Thus it is clear that the present experiment leads to the first reliable determination of the spectral shape and absolute flux of atmospheric gamma rays near the top of the atmosphere in the energy range 40–1000 GeV.

3.2. *The Production spectrum of gamma rays at the top of the atmosphere*

Gamma rays observed at balloon altitudes contain, in principle, contributions from these sources: (i) those produced through nuclear interactions of primary cosmic rays with atmospheric nuclei; (ii) those radiated by primary electrons; and (iii) primary cosmic gamma rays. It is now generally acknowledged that the flux of gamma rays of primary origin is negligible for our purpose. Gamma rays radiated by primary electrons during their propagation in the atmosphere can be evaluated using the observed flux of primary electrons and the relevant bremsstrahlung cross-section. Since there is an indication of a steepening of the primary electron spectrum beyond about 150 GeV (Anand *et al* 1971), we have separately calculated the radiated gamma rays by making use of the electron spectrum given by Anand *et al* (1968) to continue up to 1000 GeV and also assuming a steepening beyond 150 GeV by one power. It is then found that even the mean of these estimates is only about 10 per cent of the observed flux values; the uncertainty in this estimated flux is about 5 per cent of the observed value at 1000 GeV which decreases to about 2 per cent around 50 GeV. After subtracting the estimated contribution due to gamma rays radiated by primary electrons from the observed flux, the production spectrum at the top of the atmosphere through interactions of cosmic ray nuclei is given by

$$P_\gamma\,(E, 0) = \mathcal{J}_\gamma'\,(E, x)/47{\cdot}1\,f(x) \qquad (4)$$

where $\mathcal{J}_\gamma'(E)$ is the corrected flux of gamma rays. In figure 6, we have shown on the right hand side the production spectrum of gamma rays in units of photons $g^{-1}sr^{-1}sec^{-1}$ GeV^{-1}. This spectrum can be represented by a power law of the type:

$$P_\gamma(E, 0) = 8{\cdot}02 \times 10^{-4} E^{-2{\cdot}60 \pm 0{\cdot}09} \text{ photons (g sr sec GeV)}^{-1} \qquad (5)$$

A comparison of this spectrum with that determined below 30 GeV (Stephens 1970a) shows that while the spectral index is the same, the absolute intensity above 40 GeV is about a factor of two, larger than that expected by simply extrapolating the spectrum obtained at low energies. One possible explanation offered (Stephens 1970b) for this apparent increase in the flux of gamma rays at high energies is a change in the characteristics of high energy interactions at primary energies greater than a few hundred GeV.

3.3. *Secondary electrons in the Atmosphere*

At energies greater than a few GeV, the atmospheric electrons are mainly due to the electromagnetic cascading of gamma rays produced in the atmosphere (Stephens 1969; Daniel and Stephens 1970). Thus knowing the gamma ray production spectrum given by equation 5, whose dependence with depth is proportional to $\exp(-x/\Lambda)$, where $\Lambda=125$ g cm^{-2} the attenuation length of cosmic ray nuclei, we can calculate the secondary electron component at any depth using the relations given by Nishimura (1967). We write the flux due to secondary electrons as follows:

$$\mathcal{J}_e(E, x) = 1{\cdot}69\times10^2E^{-2{\cdot}6}\{7{\cdot}644\exp(-x/125{\cdot}0) - 8{\cdot}20\exp(-x/94{\cdot}4) + 0{\cdot}556\exp(-x/21{\cdot}64)\} \text{ electrons/(m}^2\text{ sr sec GeV)} \quad (6a)$$

and

$$\mathcal{J}_\gamma(E, x) = 3{\cdot}78\times10^2E^{-2{\cdot}6}\{6{\cdot}069\exp(-x/125{\cdot}0) - 5{\cdot}914\exp(-x/94{\cdot}4) - 0{\cdot}155\exp(-x/21{\cdot}64)\} \text{ photons/(m}^2\text{ sr sec GeV)} \quad (6b)$$

One can see from equations 6a and 6b that the secondary atmospheric electron flux is only about 6 per cent of the gamma ray flux at 10 g cm^{-2} increasing to 10·5 per cent at 16 g cm^{-2}. Thus we are able to demonstrate here that a study of the gamma ray spectrum using the same detector as that meant for the primary cosmic ray electrons, provides the most reliable method of estimating the contribution of atmospheric secondary electrons in the sample of observed electrons.

Acknowledgement

We are thankful to Prof. G S Gokhale, Mr R T Redkar and the balloon crew of the Institute for the balloon flight, to Mr P J Kajarekar for the processing of emulsions, to Mr M V Patel for the fabrication of the assembly and to Mrs S M Adhikari, Mrs Prabhu Desai, Miss S Savitri and Miss P H Umadikar for the painstaking microscope work.

References

Abraham F, Kidd J, Koshiba M, Levi Setti R, Tsao C H and Wolter W 1963a, *Nuovo Cimento* **28** 221; 1963b *Nuovo Cimento* **29** 315

Anand K C, Daniel R R and Stephens S A 1968 *Phys. Rev. Lett.* **20** 764

Anand K C, Daniel R R and Stephens S A 1970 *Acta Phys. Acad. Sci. Hung.* **29**, Suppl. 1, 229

Anand K C, Daniel R R and Stephens S A 1971 *Proc. Twelfth Int. Conf. Cosmic Rays, Hobart* HE–55.

Anand K C, Daniel R R and Stephens S A 1971 *Proc. Twelfth Int. Conf. Cosmic Rays, Hobart* OG–39

Anand K C and Stephens S A 1971 *Proc. Twelfth Int. Conf. Cosmic Rays, Hobart* HE–59

Daniel R R and Stephens S A 1970 *Space Sci. Rev.* **10** 599

Duthie J, Fowler P H, Kaddoura A, Perkins D H and Pinkau K 1962 *Nuovo Cimento* **24** 122

Kidd J 1963a *Nuovo Cimento* **27** 57; 1963b *Nuovo Cimento* **29** 315

Kidd J and Nishimura J 1964, *Nuovo Cimento Suppl.* **1** 1039

Malhotra P K, Shukla P G, Stephens S A, Vijayalakshmi B, Boult J, Bowler M G, Fowler P H, Hackforth H L, Keereetaveep J, Mayes V M and Tovey S N 1965 *Nuovo Cimento* **40** 385

Nishimura J 1967 ' Theory of Cascade Showers ' in *Handbuch der Physik* Vol. XLVI/2 ed K Sitte (Berlin: Springer–Verlag) pp 1-114

Stephens S A 1969, Ph.D. thesis, University of Bombay

Stephens S A 1970a *Proc. Indian Acad. Sci. Sect. A* **72** 214

Stephens S A 1970b *Acta. Phys. Acad. Sci. Hung.* **29** *Suppl. 2* 773

Nishumura J, Mikumo E, Mito I, Niu K, Ohta I and Taira T 1970 *Acta. Phys. Acad. Sci. Hung.* **29** *Suppl. 1* 239